Supplemental Information for

CRH engagement of the locus coeruleus noradrenergic system mediates stress-induced anxiety

Jordan G. McCall,[1,2,3,4] Ream Al-Hasani,[1,2,3] Edward R. Siuda,[1,2,3,4] Daniel Y. Hong[1], Aaron J. Norris[1], Christopher P. Ford[5], Michael R. Bruchas[1,2,3,4*]

[1]Department of Anesthesiology, Division of Basic Research, Washington University School of Medicine, St. Louis, MO 63110, USA.

[2]Washington University Pain Center, Washington University School of Medicine, St. Louis, MO 63110, USA.

[3]Department of Anatomy & Neurobiology, Washington University School of Medicine, St. Louis, MO 63110, USA.

[4]Division of Biological & Biomedical Sciences, Washington University School of Medicine, St. Louis, MO 63110, USA.

[5]Department of Physiology & Biophysics, Department of Neurosciences, Case Western Reserve University School of Medicine, Cleveland, OH 44106, USA

*To whom correspondence should be addressed.

E-mail: bruchasm@wustl.edu

Michael R. Bruchas, PhD

This Word file includes:

Figures S1-S7
Figure Legends for Figures S1-S7
Extended Experimental Procedures
Movie Legends for Movie S1
Supplemental References

Other Supplementary Materials for this manuscript includes the following:

Movies S1

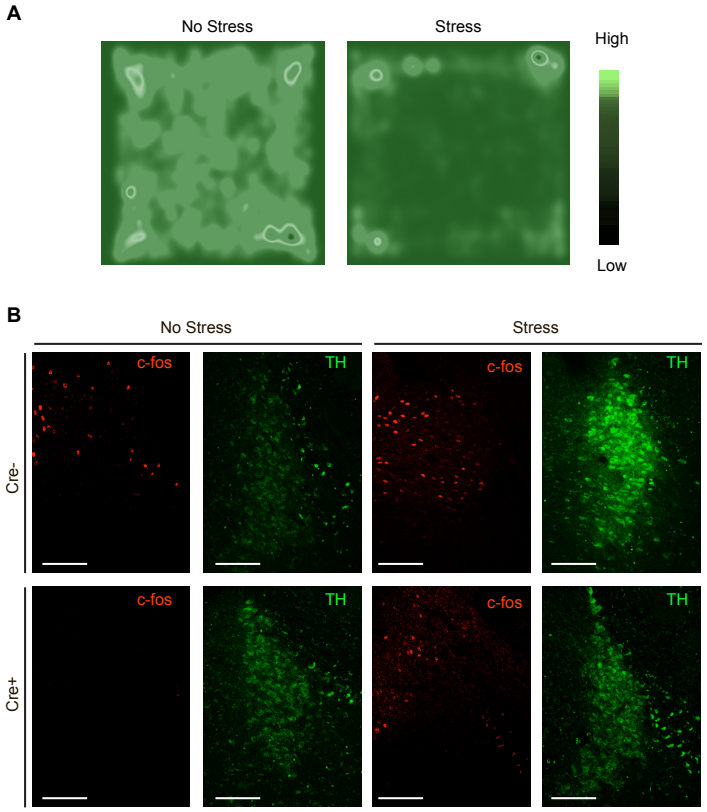

Figure S1: Related data to Figure 1A-D (**A**) Representative heat maps of activity during WT OFT. (**B**) Separated channels from representative immunohistochemistry shown in **Fig. 1G.** hM4Di inhibition of LC neurons decreases c-fos immunoreactivity in LC neurons (Red=c-fos, green=tyrosine hydroxylase, Scale bars= 100 µm. (**C**) Inhibition of LC-NE neurons during stress blocks stress-induced anxiety as seen in entries into the center of the OFT. Data represented as mean ± SEM, n=8-13/group: One-Way ANOVA, Newman-Keuls post-hoc, No stress/Cre- vs. No stress/Cre+, not significant, No stress/Cre- vs. Stress/Cre- **p<0.01, No stress/Cre- vs. Stress/Cre+, not significant, No stress/Cre+ vs. Stress/Cre- **p<0.01, No stress/Cre+ vs. Stress/Cre+, not significant).

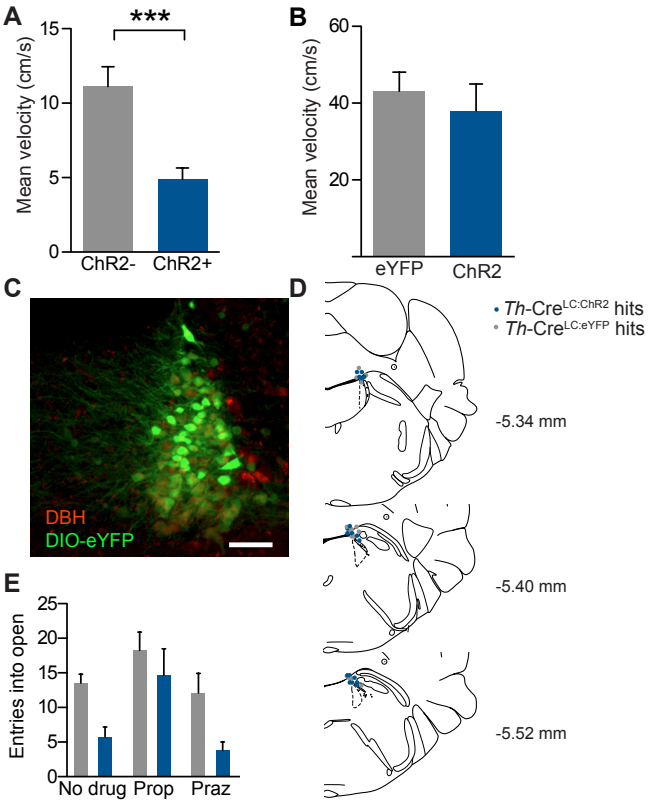

Figure S2: High tonic LC-NE neuronal activity is sufficient to induce anxiety-like behavior. Related data to Figure 3. (**A**) There is also a change in mean velocity during the OFT of previously photostimulated mice. Data represented as mean ± SEM, ***<0.001, n=14-15/group. (**B**) There is also no change in mean velocity during the photostimulation in the OFT. Data represented as mean ± SEM, n=10/group. (**C**) Representative immunohistochemistry shows selective targeting of AAV5-DIO-eYFP to DBH+ LC neurons of Th-Cre$^{LC:eYFP}$ controls (Red= dopamine beta hydroxylase, green=DIO-eYFP, scale bars= 100 µm. (**D**) Fiber optic tip placements for the OFT and EZM experiments. Animals were excluded if the tip ended >1 mm dorsal of the LC or any caused significant lesion to the LC or 4th ventricle. For clarity, only hits of included mice for this experiment are shown.

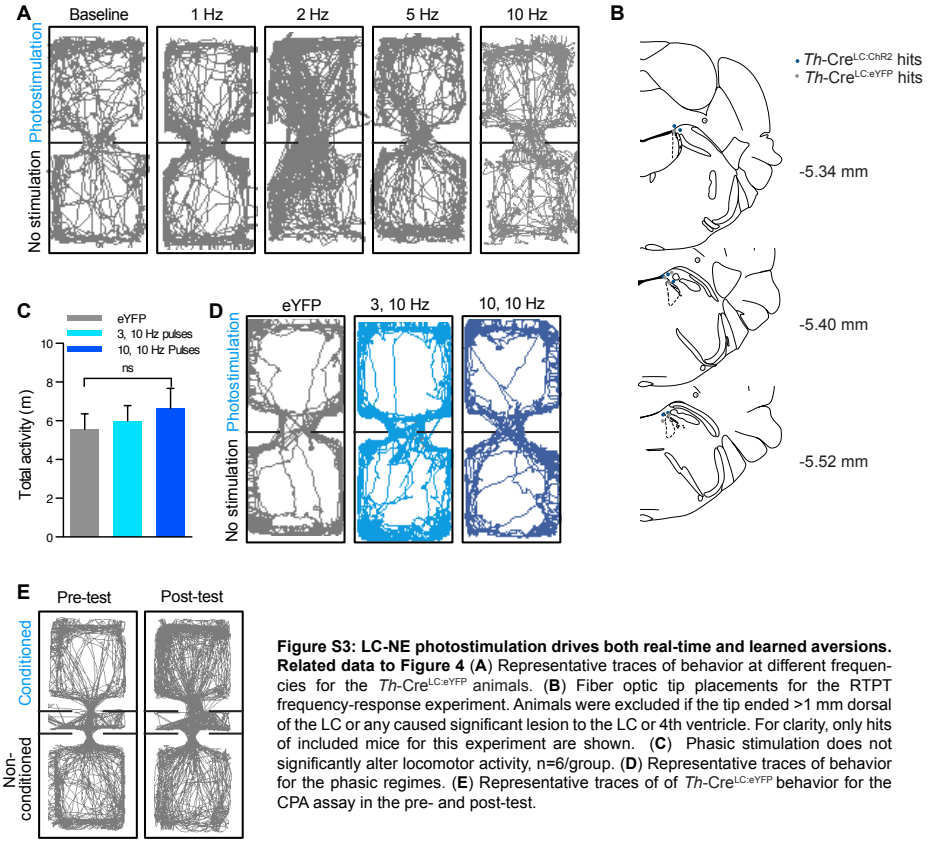

Figure S3: LC-NE photostimulation drives both real-time and learned aversions. Related data to Figure 4 (**A**) Representative traces of behavior at different frequencies for the *Th*-Cre$^{LC:eYFP}$ animals. (**B**) Fiber optic tip placements for the RTPT frequency-response experiment. Animals were excluded if the tip ended >1 mm dorsal of the LC or any caused significant lesion to the LC or 4th ventricle. For clarity, only hits of included mice for this experiment are shown. (**C**) Phasic stimulation does not significantly alter locomotor activity, n=6/group. (**D**) Representative traces of behavior for the phasic regimes. (**E**) Representative traces of of *Th*-Cre$^{LC:eYFP}$ behavior for the CPA assay in the pre- and post-test.

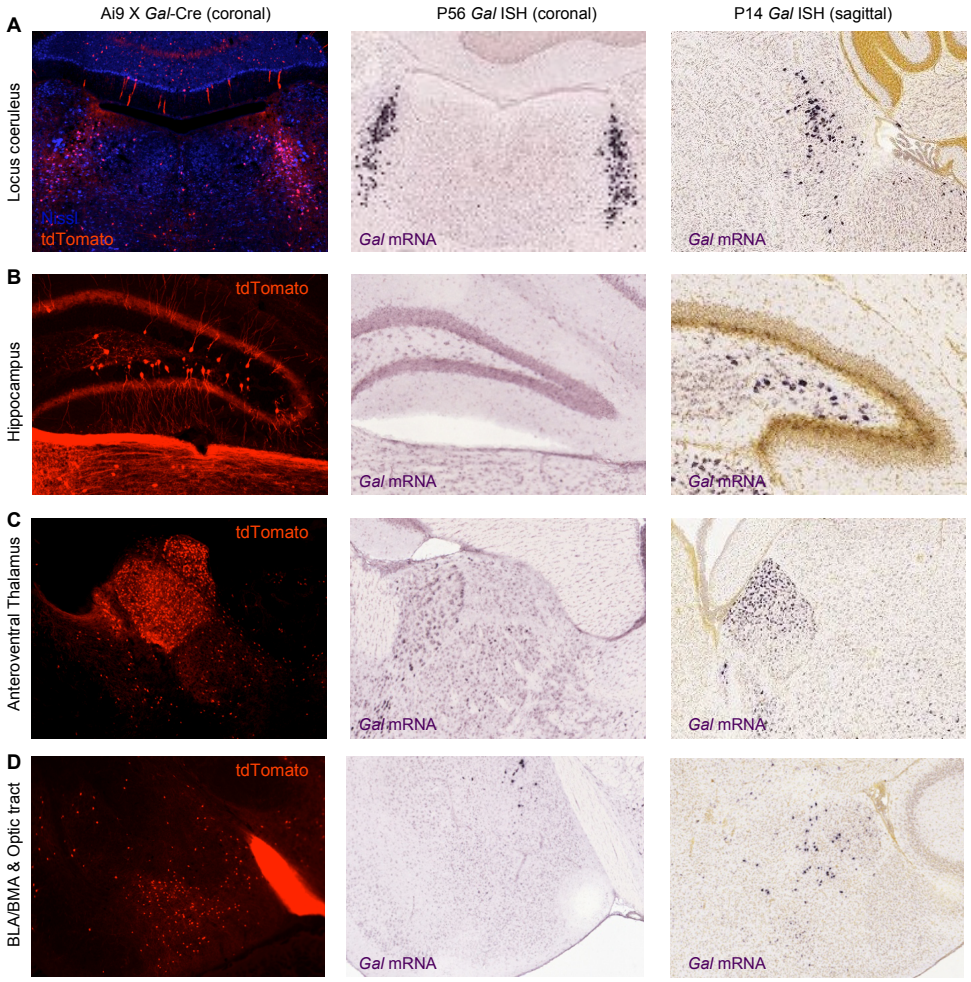

Figure S4: Cre-dependent tdTomato expression in adult Ai9 X *Gal*-Cre mice. Related data to Figure 5A & B. (**A**) Images show Cre-dependent reporter expression in adult Ai9 X Gal-Cre mice (left panel), *in situ* hybridization for *Gal* in adult WT mice from the Allen Institute (middle panel), and *in situ* hybridization for *Gal* in P14 WT mice from the Allen Institute (right panel) for the (**A**) locus coeruleus, (**B**) hippocampus, (**C**) anteroventral thalamus, and (**D**) basolateral and basomedial amygdala. We did observe any regions that contain Cre-dependent reporter expression that were not positive for *Gal* mRNA at some stage in development or in the adult animal.

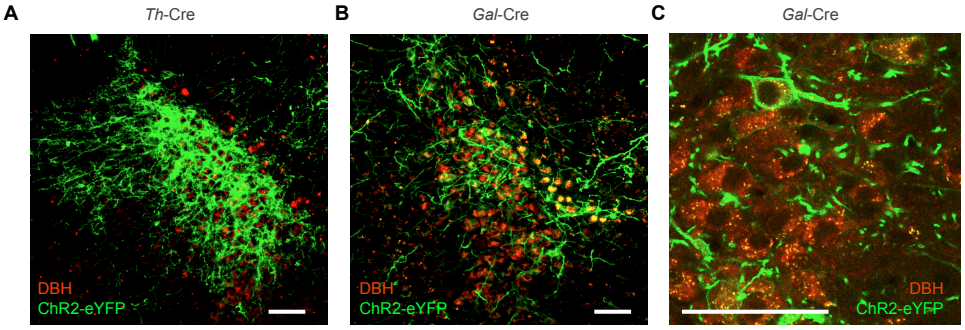

Figure S5: *Gal*-Cre mice can be used to effectively target a subset of LC neurons. Related data to Figure 5D&E. (**A**) Representative immunohistochemistry show selective targeting of ChR2-eYFP to DBH+ LC neurons in *Th*-Cre mice (Red= tyrosine hydroxylase, green=ChR2-eYFP, Scale bars= 100 µm). (**B**) Representative immunohistochemistry show selective targeting of ChR2-eYFP to a subset of DBH+ LC neurons in *Gal*-Cre mice (Red= tyrosine hydroxylase, green=ChR2-eYFP, Scale bars= 100 µm).(**C**) High-power confocal micrograph depicting ChR2-eYFP membrane labeling in *Gal*-Cre DBH+ neurons.

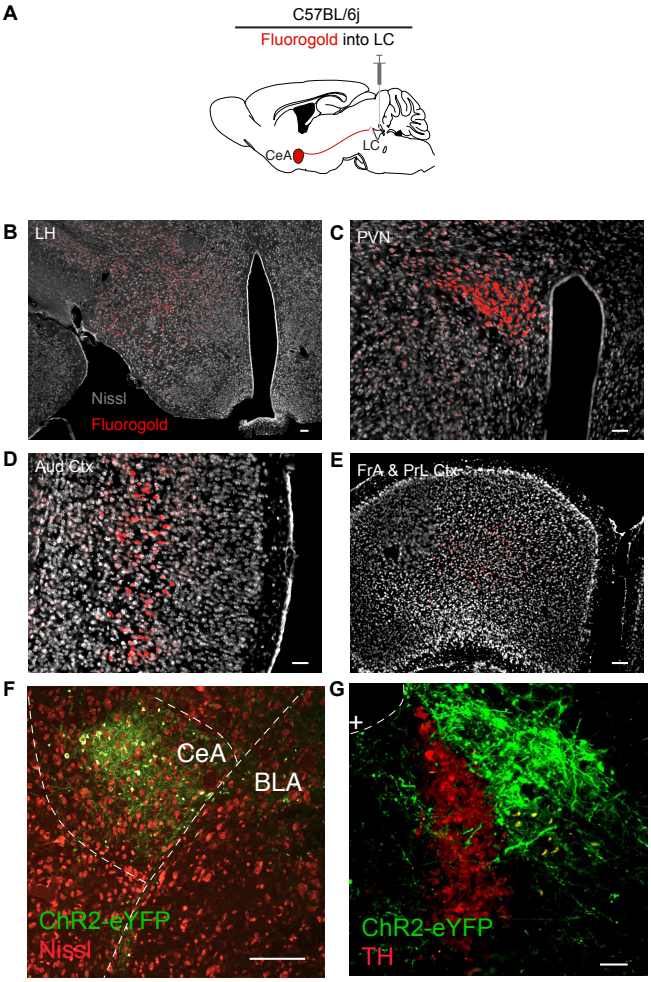

Figure S6: Retrograde fluorogold labeling in various forebrain regions and anterograde viral labeling. Related data to Figure 6 (**A**) Cartoon depicting fluorgold tracing strategy. Representative images shows retrograde labeling throughout in the (**B**) lateral hypothalamus (LH), (**C**) paraventricular nucleus of the hypothalamus (PVN), (**D**) auditory cortex (Aud Ctx), and (**E**) frontal association (FrA) and prelimbic cortex (PrL Ctx) paraventricular nucleus of the hypothalamus. In all images, fluorogold is psuedocolored red and Nissl is in grey. All scale bars are 100 µm. (**F** and **G**) Coronal images depict robust eYFP labeling in the CeA and LC of the same mouse. All scale bars are 100 µm. + is in 4th ventricle.

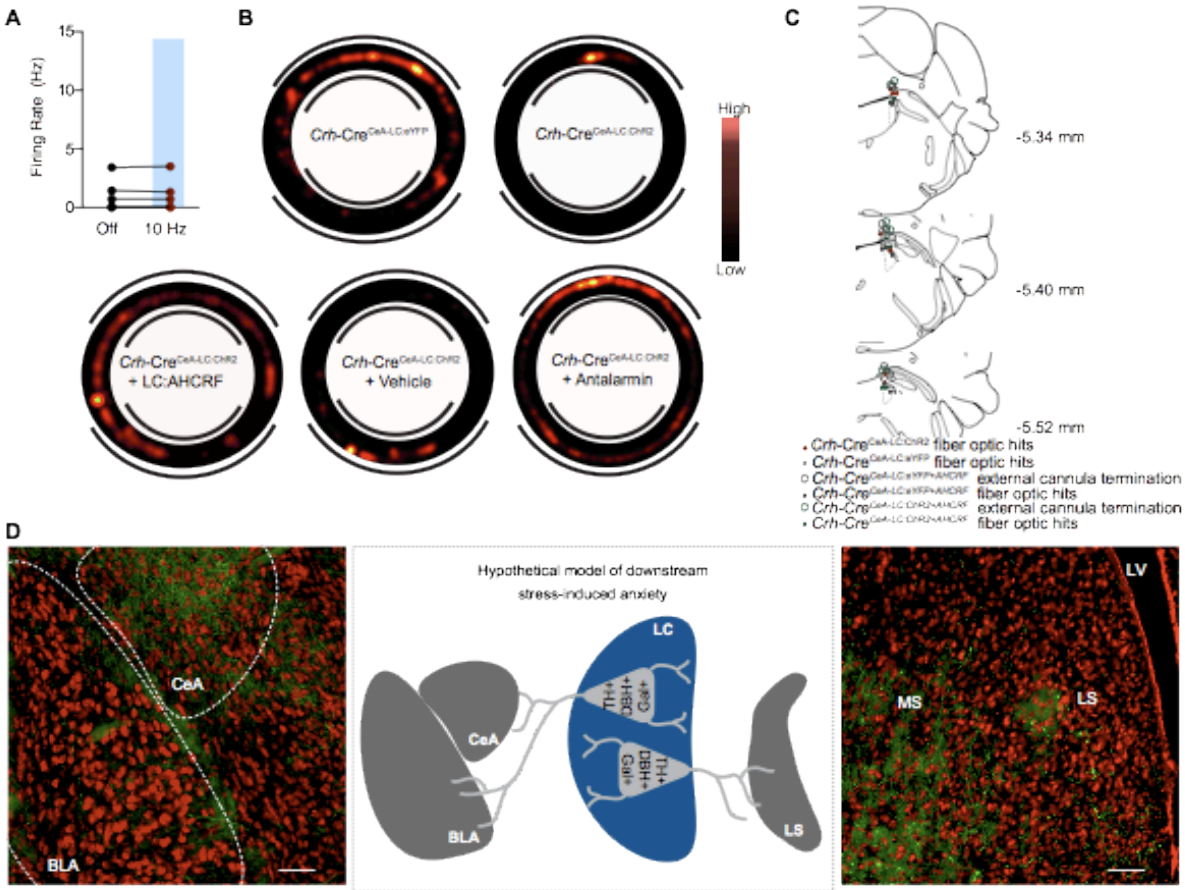

Figure S7: CRH+ CeA-LC terminals increase LC activity and drive anxiety through CRFR1 activation. Related data to Figures 7 & 8. (**A**) n=5 units that did not increase or decrease firing by >10% during 10 Hz photostimulation. (**B**) Representative heat maps of activity in the EZM. (**C**) Cannula and fiber optic tip placements for the EZM experiments with *Crh*-Cre$^{CeA\text{-}LC}$ animals. Animals were excluded if the fiber tip ended >1 mm dorsal of the LC or any caused significant lesion to the LC or 4th ventricle. Additionally, cannulated mice were excluded if the final injection placement appeared to be >0.5 mm from the LC. For clarity, only hits of included mice for this experiment are shown. (**D**) Hypothetical model of downstream LC-NE influence on anxiety-like behaviors. Anterograde tracing of eYFP+ fibers from Th-Cre$^{LC:eYFP}$ mice reveals dense innervation in the CeA, BLA, and LS. (red= Nissl, green=DIO-eYFP, scale bars= 100 µm).

Extended Experimental Procedures

Experimental subjects & Stereotaxic surgery

Adult (25–35 g) male C57BL/6J, *TH*-IRES-Cre, *Crh*-IRES-Cre, and *Gal*-Cre (all backcrossed to C57BL/6J mice for ~10 generations) were group-housed, given access to food pellets and water *ad libitum* and maintained on a 12 h:12 h light:dark cycle (lights on at 7:00 AM). Animals were held in a sound attenuated holding room facility in the lab 1 week prior to surgery, post-surgery and throughout the duration of the behavioral assays to minimize stress from transportation and disruption from foot traffic. All mice were handled and, where appropriate, connected to fiber optics and/or tubing two times a day for one week prior to experimental testing. All procedures were approved by the Animal Care and Use Committee of Washington University and conformed to US National Institutes of Health guidelines.

Stereotaxic surgery

After the animals were acclimated to the holding facility for seven to nine days, they were anaesthetized in an induction chamber (4% Isolflurane) and placed in a stereotaxic frame (Kopf Instruments, Model 1900) where they were maintained at 1-2% isoflurane. A craniotomy was performed and mice were injected with 500 nl of AAV5-DIO-HM4Di, AAV5-DIO-ChR2 or AAV5-DIO-eYFP, Fluorogold, or CTB-594 unilaterally into the LC (stereotaxic coordinates from bregma: -5.45 anterior-posterior (AP), +/−1.25 medial-lateral (ML), −4.00 mm dorsal-ventral (DV)), or the CeA (-1.25 AP, +/- 2.75 ML, -4.75 DV). Mice were then implanted with metal cannula (PlasticsOne; coordinates adjusted from viral injection 0.00 AP, +/- 0.25 ML, +1.00 DV) or fiber optic implants (coordinates adjusted from viral injection 0.00 AP, +/- 0.25 ML, +1.00 DV)(Carter et al., 2010). Custom adapters (WUSTL Instrument Machine Shop) for the Kopf cannula holder (Model 1966) were used to implant the fiber optics(Sparta et al., 2011). The implants were secured using two bone screws (CMA, 743102) and affixed with dental cement

(Lang Dental). Mice were allowed to recover for 3-6 weeks prior to behavioral testing; this interval also permitted optimal AAV expression and Cre recombinase activity.

Viral preparation

Plasmids coding pAAV-EF1α-DIO-EFYP and pAAV-EF1α-double floxed-hChR2(H134R)-EYFP-WPRE-HGHpA, were obtained from Addgene (Addgene.org) originally from the Deisseroth Laboratory at Stanford University. The DNA was amplified with a Maxiprep kit (Promega) and packaged into AAV5 serotyped viruses by the WUSTL Hope Center Viral Core. The final viral concentration was 2-5 x 1012 genome vg/mL for the adeno-associated viruses. AAV5-EF1α-DIO-HM4Di-mCherry was purchased directly from the UNC Vector Core.

Plasmid	**Source**	**Packaged by**	**Serotype**	**Titer**
pAAV-EF1α-DIO-EFYP	Deisseroth Laboratory (Stanford)	WUSTL Hope Center Viral Core	AAV5	5 x 10^12 vg/ml
pAAV-EF1α-double floxed-hChR2(H134R)-EYFP-WPRE-HGHpA	Deisseroth Laboratory (Stanford)	WUSTL Hope Center Viral Core	AAV5	2 x 10^13 vg/ml
AAV5-EF1α-DIO-HM4Di-mCherry	Roth Laboratory (UNC)	UNC Vector Core	AAV5	3x10^12 VM/mL

Stress-induced anxiety paradigm

Mice assigned to stress groups were restrained in 50 ml disposable conical tubes that were adapted for this purpose by drilling holes to permit air circulation and for the tail to be extended. For acute stress-induced anxiety-like behavior, mice were immobilized in the tube once for 30 minutes (Chmielarz et al., 2013; Schaefer et al., 2000; Sim et al., 2013). Immediately following stress, animals were transferred to the open field (see below). Fecal boli were collected from both the tube and the open field. For the hM4Di experiments, mice were injected with CNO (10 mg/kg, i.p., 30 min prior to exposure to the restraint tube) (Armbruster et al., 2007; Li et al., 2013; Mahler et al., 2014; Penzo et al., 2015; Vazey and Aston-Jones, 2014). For the CRF antagonism experiment, mice were injected with Antalarmin HCl (10 mg/kg, i.p., 30 min prior to exposure to the restraint tube).

Open Field Test (OFT)

OFT testing was performed in a square enclosure (50 x 50 cm) within a sound attenuated room maintained at 23ºC. Lighting was measured and stabilized at ~25 lux. For stress-induced experiments, we followed the above paradigm immediately prior to a 20 minute test. For optogenetic experiments, we connected *Th*-Cre$^{LC:ChR2}$ or *Th*-Cre$^{LC:eYFP}$ mice to fiber optic cables and placed them in the center of the open field and allowed them to roam freely for 21 min. Photostimulation alternated between off and on states in 3 min time segments, beginning with 3 min of no stimulation. For the photostimulated time segments, animals received 5 Hz (10 ms width) photostimulation (~10 mW light power). The open field was cleaned with 70% ethanol between each trial. Movements were video recorded and analyzed using Ethovision 8.5 (Noldus Information

Technologies, Leesburg, VA). The center was defined as a square comprised of 50% the total area of the OFT. Time in the center was the primary measure of anxiety-like behaviors.

Elevated Zero Maze (EZM)

EZM testing was performed in a sound attenuated room maintained at 23ºC at 200 lux(Bruchas et al., 2009; Kim et al., 2013b), and trials were performed in the afternoon between 13:00–16:00 hr. The EZM (Harvard Apparatus, Holliston, MA) had the following dimensions: 200 cm in circumference comprised of four 50 cm sections: two opened and two closed. The maze was elevated 50 cm above the floor, with a path width of 4 cm and a 0.5 cm lip on each open section. The maze was cleaned with 70% ethanol between trials. Prior to testing, *Th*-Cre$^{LC:ChR2}$, *Th*-Cre$^{LC:eYFP}$, *Crh*-Cre$^{CeA\text{-}LC:ChR2}$, or *Crh*-Cre$^{CeA\text{-}LC:eYFP}$ were connected to the fiber optic and placed at the threshold of a closed section facing the open section and allowed to roam freely for 7 min. *Th*-Cre animals received 5 Hz (10 ms width) and *Crh*-Cre animals received 10 Hz (10 ms width) photostimulation (~10 mW light power). For α_1- and β–adrenergic antagonism, mice were injected with saline vehicle, Propranolol (10 mg/kg, i.p, Tocris) (Al-Hasani et al., 2013; Shanks et al., 1966) or Prazosin (1 mg/kg, Sigma) (Bortolozzi and Artigas, 2003; Graham et al., 1977) 30 minutes prior to behavior (Bortolozzi and Artigas, 2003; Al-Hasani et al., 2013). For the CRFR1 antagonism experiments, mice were injected into the LC with α-helical CRF (1 µg, intra-LC, one hour prior to behavior, Tocris) or Antalarmin HCl (10 mg/kg, i.p., 30 min prior to behavior, Sigma). Movements were video recorded and analyzed using Ethovision 8.5 (Noldus Information Technologies,

Leesburg, VA). Open section time and entries into the open section following a one-minute habituation were the primary measures of anxiety-like behaviors.

Real-time Place Testing

Animals were placed in a custom-made unbiased, balanced two-compartment conditioning apparatus (52.5 x 25.5 x 25.5 cm) as described previously (Jennings et al., 2013; Kim et al., 2013a; Siuda et al., 2015; Stamatakis and Stuber, 2012; Stamatakis et al., 2013; Tan et al., 2012). Mice were allowed to freely roam the entire apparatus for 20 min. Entry into one compartment triggered photostimulation of various frequencies (0, 1, 2, 5, 10 Hz, etc.) while the animal remained in the light-paired chamber. Entry into the other chamber ended the photostimulation. For α_1- and β–adrenergic antagonism, mice were injected with saline vehicle, Propranolol (10 mg/kg, i.p, Tocris) (Al-Hasani et al., 2013; Shanks et al., 1966) or Prazosin (1 mg/kg, Sigma) (Bortolozzi and Artigas, 2003; Graham et al., 1977) 30 minutes prior to behavior.

Conditioned Place Aversion

Th-Cre$^{LC:ChR2}$, *Th*-Cre$^{LC:eYFP}$, *Crh*-Cre$^{CeA\text{-}LC:ChR2}$, or *Crh*-Cre$^{CeA\text{-}LC:eYFP}$ animals were trained in an unbiased, balanced three-compartment conditioning apparatus as described (Bruchas et al., 2009; Al-Hasani et al., 2013; Land et al., 2008, 2009). Briefly, mice were pre-tested by placing individual animals in the small central compartment and allowing them to explore the entire apparatus for 30 min. Time spent in each compartment was recorded with a video camera (ZR90; Canon) and analyzed using Ethovision 8.5 (Noldus). Mice were randomly assigned to photostimulation and no-photostimulation compartments and received no photostimulation in the morning and photostimulation (*Th*-Cre$^{LC:ChR2}$: 5 Hz, 10 ms pulses; *Crh*-Cre$^{CeA\text{-}LC:ChR2}$: 10 Hz, 10

ms pulses) in the afternoon at least 4 h after the morning training on two consecutive days. CPA was assessed on day 4 by allowing the mice to roam freely in all three compartments and recording the time spent in each. Scores were calculated by subtracting the time spent in the photostimulation-paired compartment post-test minus the pre-test.

Immunohistochemistry

Immunohistochemistry was performed as described (Al-Hasani et al., 2013; Kim et al., 2013b). Briefly, mice were anesthetized with pentobarbital and transcardially perfused with ice-cold 4% paraformaldehyde in phosphate buffer (PB). Brains were dissected, post-fixed for 24 hr at 4 ºC and cryoprotected with solution of 30% sucrose in 0.1M PB at 4ºC for at least 24 hr, cut into 30 µm sections and processed for immunostaining. 30 µm brain sections were washed three times in PBS and blocked in PBS containing 0.5% Triton X-100 and 5% normal goat serum. Sections were then incubated for ~16 hr at room temperature in rabbit anti c-fos antibody (1:500, Santa Cruz), rabbit anti-DBH (1:2000, Millipore) and/or chicken anti-TH (1:2000, Aves Labs). Following incubation, sections were washed three times in PBS and then incubated for 2 hr at room temperature in Alexa Fluor 488 goat anti-mouse IgG (1:500, Invitrogen), Alexa Fluor 594 goat anti-rabbit IgG (1:500, Invitrogen), and/or goat anti-chicken Alexa Fluor 633(1:500, Invitrogen) were then washed three times in PBS and followed by three 10-min rinses in PB and mounted on glass slides with Hardset Vectashield (Vector Labs) for microscopy. All sections were imaged on both epifluorescent and confocal microscopes. Gain and exposure time were constant throughout each experiment, and all image groups were processed in parallel using Adobe Photoshop CS5 (Adobe Systems). IHC was quantified as previously described (Al-Hasani et al., 2013; Kim et al., 2013b). Briefly, channels were separated, an exclusive threshold was set, and positive staining for each channel was counted in a blind-to-treatment fashion using Metamorph. The counts from each channel were then overlaid and percent of co-labeled cells were reported.

Antibody	Species	Dilution	Source
TH	Chicken	1:2000	Aves Labs
c-fos	Rabbit	1:500	Santa Cruz
DBH	Rabbit	1:2000	Millipore
Alexa Fluor 488 anti-mouse IgG	Goat	1:500	Invitrogen
Alexa Fluor 594 anti-rabbit IgG	Goat	1:500	Invitrogen
Alexa Fluor 633 anti-chicken IgG	Goat	1:500	Invitrogen
Alexa Fluor 594 anti-chicken IgG	Goat	1:500	Invitrogen

Anatomical tracing

For retrograde tracing experiments (Fluorogold and CTB-594), the tracer was injected and the animal was allowed to recover for six days before perfusion. For anterograde viral tracing, the virus was injected and the animal was allowed to recover for six weeks before perfusion.

Slice electrophysiology preparation and solutions

Following anesthesia, horizontal midbrain slices containing the LC (240 µm) were cut in ice-cold sucrose cutting solution that contained (mM): 75 NaCl, 2.5 KCl, 6 $MgCl_2$, 0.1 $CaCl_2$, 1.2 NaH_2PO_4, 25 $NaHC0_3$, 2.5 D-glucose, 50 sucrose; bubbled with 95% O_2/5% CO_2. Slices were incubated post-cutting at 35°C in oxygenated 95% O_2/5% CO_2 ACSF solution that contained (mM): 126 NaCl, 2.5 KCl, 1.2 $MgCl_2$, 2.5 $CaCl_2$, 1.2 NaH_2PO_4, 21.4 $NaHCO_3$, 11.1 D-glucose for

45 minutes before recording. During incubation, 10 μM MK-801 was included to reduce excitotoxicity and increase slice viability. Following incubation, slices were placed in a recording chamber and constantly perfused with warm ACSF (34 ± 2°C) containing 100 μM picrotoxin, 10 μM DNQX and 1 μM idazoxan at 2 ml/min. Neurons were visualized with a BXWI51 microscope (Olympus) with infrared custom-built gradient contrast optics.

Slice electrophysiology

Whole-cell current-clamp recordings were made as described (Courtney and Ford, 2014) using an Axopatch 200B amplifier (Molecular Devices). Data was acquired using an ITC-18 interface (Instrutech) and Axograph X (Axograph Scientific) at 10 KHz and filtered to 2 KHz for voltage-clamp recordings. Widefield activation of ChR2 was activated with collimated light from a LED (470 nm, ~1 mW) through the 40x water immersion objective. Patch pipettes (1.5-2 MW) were pulled from borosilicate glass (World Precision Instruments). For whole cell recordings of ChR2 currents and action potentials in LC neurons the extracellular solution contained 100 mM picrotoxin, 10 μM DNQX and 1 μM idazoxan, and the intracellular pipette solution contained 115 mM K-methylsulphate, 20 mM NaCl, 1.5 mM MgCl2, 10 mM HEPES(K), 10 mM BAPTA-tetrapotassium, 1mg/ml ATP, 0.1 mg/ml GTP, and 1.5 mg/ml phosphocreatine (pH 7.4, 275 mOsm). To examine potential synaptic events driven by optogenetic stimulation of CRH terminals in the LC, recordings were made in the absence of synaptic receptor antagonists and the intracellular pipette solutions contained 58 mM K-methylsulphate, 58 mM KCl, 20 mM NaCl, 1.5 mM MgCl2, 10 mM HEPES(K), 0.1 mM EGTA, 1mg/ml ATP, 0.1 mg/ml GTP, and 1.5 mg/ml phosphocreatine (pH 7.4, 275 mOsm). Flash pulses were 3 ms. To confirm that photostimulation of terminals arising from the CeA did not evoke measurable synaptic events,

recordings were also made in a subset of trials (n = 5) in the presence of TTX (500 nM), 4-AP (100 μM) and antalarmin (10 μM).

Genotyping of mouse lines

DNA was isolated from tail tissue obtained from weanling mice (21-28 days of age), and PCR screening was performed using the following primers: Cre recombinase (forward: 5'- GCA TTA CCG GTC GAT GCA ACG AGT GAT GAG-3' and reverse: 5'- GAG TGA ACG AAC CTG GTC GAA ATC AGT GCG-3') yielding a 400-bp PCR product in Cre positive animals. Fatty acid-binding protein intestinal primers (forward: 5'- TGG ACA GGA CTG GAC CTC TGC TTT CCT AGA-3' and reverse: 5'- TAG AGC TTT GCC ACA TCA CAG GTC ATT CAG-3') were used as positive controls and yield a 200-bp PCR product.

Supplemental Movie Legend

Movie S1. Animated confocal z-stack illustrating *Crh*$^{+}$ innervation (eYFP; green) medial and lateral to as well as within LC-NE neurons (DBH; red).

Supplemental References

Al-Hasani, R., McCall, J.G., Foshage, A.M., and Bruchas, M.R. (2013). Locus Coeruleus Kappa Opioid Receptors modulate Reinstatement of Cocaine Place Preference through a Noradrenergic Mechanism. Neuropsychopharmacology.

Armbruster, B.N., Li, X., Pausch, M.H., Herlitze, S., and Roth, B.L. (2007). Evolving the lock to fit the key to create a family of G protein-coupled receptors potently activated by an inert ligand. Proc. Natl. Acad. Sci. U. S. A. *104*, 5163–5168.

Bortolozzi, A., and Artigas, F. (2003). Control of 5-hydroxytryptamine release in the dorsal raphe nucleus by the noradrenergic system in rat brain. Role of alpha-adrenoceptors. Neuropsychopharmacol. Off. Publ. Am. Coll. Neuropsychopharmacol. *28*, 421–434.

Bruchas, M.R., Land, B.B., Lemos, J.C., and Chavkin, C. (2009). CRF1-R activation of the dynorphin/kappa opioid system in the mouse basolateral amygdala mediates anxiety-like behavior. PloS One *4*, e8528.

Carter, M.E., Yizhar, O., Chikahisa, S., Nguyen, H., Adamantidis, A., Nishino, S., Deisseroth, K., and de Lecea, L. (2010). Tuning arousal with optogenetic modulation of locus coeruleus neurons. Nat. Neurosci. *13*, 1526–1533.

Chmielarz, P., Kuśmierczyk, J., Parlato, R., Schütz, G., Nalepa, I., and Kreiner, G. (2013). Inactivation of Glucocorticoid Receptor in Noradrenergic System Influences Anxiety- and Depressive-Like Behavior in Mice. PLoS ONE *8*, e72632.

Courtney, N.A., and Ford, C.P. (2014). The timing of dopamine- and noradrenaline-mediated transmission reflects underlying differences in the extent of spillover and pooling. J. Neurosci. Off. J. Soc. Neurosci. *34*, 7645–7656.

Graham, R.M., Oates, H.F., Stoker, L.M., and Stokes, G.S. (1977). Alpha blocking action of the antihypertensive agent, prazosin. J. Pharmacol. Exp. Ther. *201*, 747–752.

Al-Hasani, R., McCall, J.G., Foshage, A.M., and Bruchas, M.R. (2013). Locus Coeruleus Kappa Opioid Receptors modulate Reinstatement of Cocaine Place Preference through a Noradrenergic Mechanism. Neuropsychopharmacology.

Jennings, J.H., Sparta, D.R., Stamatakis, A.M., Ung, R.L., Pleil, K.E., Kash, T.L., and Stuber, G.D. (2013). Distinct extended amygdala circuits for divergent motivational states. Nature *496*, 224–228.

Kim, S.-Y., Adhikari, A., Lee, S.Y., Marshel, J.H., Kim, C.K., Mallory, C.S., Lo, M., Pak, S., Mattis, J., Lim, B.K., et al. (2013a). Diverging neural pathways assemble a behavioural state from separable features in anxiety. Nature *496*, 219–223.

Kim, T., McCall, J.G., Jung, Y.H., Huang, X., Siuda, E.R., Li, Y., Song, J., Song, Y.M., Pao, H.A., Kim, R.-H., et al. (2013b). Injectable, Cellular-Scale Optoelectronics with Applications for Wireless Optogenetics. Science *340*, 211–216.

Land, B.B., Bruchas, M.R., Lemos, J.C., Xu, M., Melief, E.J., and Chavkin, C. (2008). The dysphoric component of stress is encoded by activation of the dynorphin kappa-opioid system. J. Neurosci. Off. J. Soc. Neurosci. *28*, 407–414.

Land, B.B., Bruchas, M.R., Schattauer, S., Giardino, W.J., Aita, M., Messinger, D., Hnasko, T.S., Palmiter, R.D., and Chavkin, C. (2009). Activation of the kappa opioid receptor in the dorsal raphe nucleus mediates the aversive effects of stress and reinstates drug seeking. Proc. Natl. Acad. Sci. U. S. A. *106*, 19168–19173.

Li, H., Penzo, M.A., Taniguchi, H., Kopec, C.D., Huang, Z.J., and Li, B. (2013). Experience-dependent modification of a central amygdala fear circuit. Nat. Neurosci. *16*, 332–339.

Mahler, S.V., Vazey, E.M., Beckley, J.T., Keistler, C.R., McGlinchey, E.M., Kaufling, J., Wilson, S.P., Deisseroth, K., Woodward, J.J., and Aston-Jones, G. (2014). Designer receptors show role for ventral pallidum input to ventral tegmental area in cocaine seeking. Nat. Neurosci. *17*, 577–585.

Penzo, M.A., Robert, V., Tucciarone, J., De Bundel, D., Wang, M., Van Aelst, L., Darvas, M., Parada, L.F., Palmiter, R.D., He, M., et al. (2015). The paraventricular thalamus controls a central amygdala fear circuit. Nature *advance online publication*.

Schaefer, M.L., Wong, S.T., Wozniak, D.F., Muglia, L.M., Liauw, J.A., Zhuo, M., Nardi, A., Hartman, R.E., Vogt, S.K., Luedke, C.E., et al. (2000). Altered Stress-Induced Anxiety in Adenylyl Cyclase Type VIII-Deficient Mice. J. Neurosci. *20*, 4809–4820.

Shanks, R.G., Wood, T.M., Dornhorst, A.C., and Clark, M.L. (1966). Some pharmacological properties of a new adrenergic beta-receptor antagonist. Nature *212*, 88–90.

Sim, H.-R., Choi, T.-Y., Lee, H.J., Kang, E.Y., Yoon, S., Han, P.-L., Choi, S.-Y., and Baik, J.-H. (2013). Role of dopamine D2 receptors in plasticity of stress-induced addictive behaviours. Nat. Commun. *4*, 1579.

Siuda, E.R., Copits, B.A., Schmidt, M.J., Baird, M.A., Al-Hasani, R., Planer, W.J., Funderburk, S.C., McCall, J.G., Gereau IV, R.W., and Bruchas, M.R. (2015). Spatiotemporal Control of Opioid Signaling and Behavior. Neuron *86*, 923–935.

Sparta, D.R., Stamatakis, A.M., Phillips, J.L., Hovelsø, N., van Zessen, R., and Stuber, G.D. (2011). Construction of implantable optical fibers for long-term optogenetic manipulation of neural circuits. Nat. Protoc. *7*, 12–23.

Stamatakis, A.M., and Stuber, G.D. (2012). Activation of lateral habenula inputs to the ventral midbrain promotes behavioral avoidance. Nat. Neurosci. *15*, 1105–1107.

Stamatakis, A.M., Jennings, J.H., Ung, R.L., Blair, G.A., Weinberg, R.J., Neve, R.L., Boyce, F., Mattis, J., Ramakrishnan, C., Deisseroth, K., et al. (2013). A unique population of ventral tegmental area neurons inhibits the lateral habenula to promote reward. Neuron *80*, 1039–1053.

Tan, K.R., Yvon, C., Turiault, M., Mirzabekov, J.J., Doehner, J., Labouèbe, G., Deisseroth, K., Tye, K.M., and Lüscher, C. (2012). GABA neurons of the VTA drive conditioned place aversion. Neuron *73*, 1173–1183.

Vazey, E.M., and Aston-Jones, G. (2014). Designer receptor manipulations reveal a role of the locus coeruleus noradrenergic system in isoflurane general anesthesia. Proc. Natl. Acad. Sci. *111*, 3859–3864.